

Evolution of magnetic states in frustrated diamond lattice antiferromagnetic $\text{Co}(\text{Al}_{1-x}\text{Co}_x)_2\text{O}_4$ spinels

O. Zaharko,^{*,1} A. Cervellino,^{1,2} V. Tsurkan,^{3,4} N. B. Christensen,^{1,5,6} and A. Loidl³

¹Laboratory for Neutron Scattering, ETHZ & PSI, CH-5232 Villigen, Switzerland

²Swiss Light Source, Paul Scherrer Institute, CH-5232 Villigen, Switzerland

³Experimental Physics V, Center for Electronics Correlations and Magnetism, University of Augsburg, D-86159 Augsburg, Germany

⁴Institute of Applied Physics, Academy of Sciences of Moldova, MD-2028 Chisinau, Republic of Moldova

⁵Materials Research Division, Risø Nat. Lab. for Sustainable Energy, Technical University of Denmark

⁶Nano-Science Center, Niels Bohr Institute, University of Copenhagen, DK-2100 Copenhagen, Denmark

(Dated: February 6, 2020)

Using neutron powder diffraction and Monte-Carlo simulations we show that a spin-liquid regime emerges at *all* compositions in the diamond-lattice antiferromagnets $\text{Co}(\text{Al}_{1-x}\text{Co}_x)_2\text{O}_4$. This spin-liquid state induced by frustration due to the second-neighbour exchange coupling J_2 , is superseded by antiferromagnetic collinear long-range order ($\mathbf{k}=0$) at low temperatures. Upon substitution of Al^{3+} by Co^{3+} in the octahedral B-site the temperature range of the spin-liquid phase narrows and T_N increases, but in contrast to previous findings, our analysis shows that the ratio J_2/J_1 remains near 0.12 for all compositions. We conclude that $\text{Co}(\text{Al}_{1-x}\text{Co}_x)_2\text{O}_4$ is just below the theoretical critical point $J_2/J_1=1/8$, and that both J_1 and J_2 increase with increasing x due to a higher efficiency of O- Co^{3+} -O as an interaction path compared to O- Al^{3+} -O.

PACS numbers: 75.50.Mm, 61.05.F-

I. INTRODUCTION

Magnetic systems with frustration induced by competing exchange interactions quite often manifest unconventional ground states, the most intriguing of which are spin-liquids¹⁵. Recently one such exotic state, a 'spiral spin-liquid', was uncovered theoretically in a classical treatment of diamond-lattice Heisenberg antiferromagnets (AFM) by Bergman *et al.*³ who showed that competition between first-neighbor J_1 and second-neighbor J_2 spin couplings creates - for $J_2/J_1 > 1/8$ - a highly degenerate ground state consisting of a set of coplanar spirals, whose propagation vectors form a continuous surface in momentum space. The frustration results in a rich phase diagram as a function of the ratio J_2/J_1 . The degeneracy of these ground states can be lifted by thermal³ or quantum⁴ fluctuations leading to an 'order-by-disorder' phase transition from a spiral spin-liquid to an ordered state.

Among the diamond-lattice AFM, compounds with the spinel structure recently attracted much attention^{5,6,7}. In particular, Co-Al oxides were considered as promising candidates for study of the 'order-by-disorder' physics^{3,4}. In these compounds of general stoichiometry AB_2O_4 the tetrahedral A-sites are occupied by high-spin ($S=3/2$) magnetic Co^{2+} ions which form a diamond lattice consisting of two interpenetrating face-centered cubic sublattices coupled antiferromagnetically. The octahedral B-sites can be filled either by nonmagnetic Al^{3+} ions and/or by low-spin ($S=0$) nonmagnetic Co^{3+} ions.

Early experiments on Co-Al oxide spinels did not provide a clear picture. A neutron-diffraction study⁸ on Co_3O_4 showed that the magnetic moments of the Co^{2+} ions

located at the tetrahedral sites form a simple collinear AFM below the Neel temperature $T_N=40$ K. This picture has been questioned by a recent μSR study⁹ which found two frequency components near T_N suggesting incommensurate magnetic order. Experimental observations on CoAl_2O_4 are also contradictory. A powder neutron diffraction study of Roth¹⁰ suggested long-range AFM order below 4 K, while Krimmel *et al.*¹¹ detected a spin liquid (or glassy-like) ground state. Electron spin resonance (ESR), magnetization and specific heat measurements identified the ground state of CoAl_2O_4 as spin-glass-like with a high frustration parameter $|T_{CW}|/T_N$ of 22 [Ref.12] and 10 [Ref.13], respectively. These experimental results are consistent with the calculations of Bergman *et al.*³ which placed CoAl_2O_4 in the region of $J_2/J_1 \approx 1/8$ where the spiral surface begins to develop. Therefore it is essential to clarify whether the ground state of Co_3O_4 is a collinear antiferromagnet and if CoAl_2O_4 is a spiral spin-liquid fluctuating among degenerate spirals. It is also important to understand why substitution within the nonmagnetic B-site changes the magnetic properties so drastically. Tristan *et al.*¹⁴ attempted to answer these questions based on bulk macroscopic measurements of $\text{Co}(\text{Al}_{1-x}\text{Co}_x)_2\text{O}_4$ system. They proposed that the spin-liquid state is realized in CoAl_2O_4 ($x=0$), while with increasing Co substitution x the second neighbor coupling J_2 decreases and collinear AFM long-range order develops.

In this work we address these important issues and refine the evolution of the magnetic states in $\text{Co}(\text{Al}_{1-x}\text{Co}_x)_2\text{O}_4$ spinels by means of neutron powder diffraction supported by Monte-Carlo simulations. Our analysis reveals that the system is very close to the critical point $J_2/J_1=1/8$

in the phase diagram remaining in the weakly frustrated limit as $J_2/J_1 \approx 0.12$. The difference in T_N and in the extent of the spin-liquid regime originate apparently from the change of the overall energy scale, i.e. the increase of the exchange coupling strength with increasing x . Polycrystalline $\text{Co}(\text{Al}_{1-x}\text{Co}_x)_2\text{O}_4$ samples with $x=0, 0.35, 0.75$ and 1 have been prepared as reported in Ref. 12. A thorough structural characterization by high-resolution x-ray synchrotron diffraction on Materials Science beamline at Swiss Light Source ($\lambda=0.41414 \text{ \AA}$) and neutron diffraction on the HRPT diffractometer at the Swiss Neutron Spallation Source SINQ ($\lambda=1.1545 \text{ \AA}$) showed no inversion for all samples, except CoAl_2O_4 . For this compound the inversion is 17% and this might influence T_N . Analyzing the lattice constants and x-ray peak profiles we concluded that the Co^{3+} ions are homogeneously and randomly distributed over the B-sites. This follows from (i) the lattice constant obeys Vegard's law¹⁵ as the function of x and (ii) there is no peak asymmetry, which would be present in the high-resolution data if any significant inhomogeneity was present.

Medium-resolution neutron powder diffraction patterns

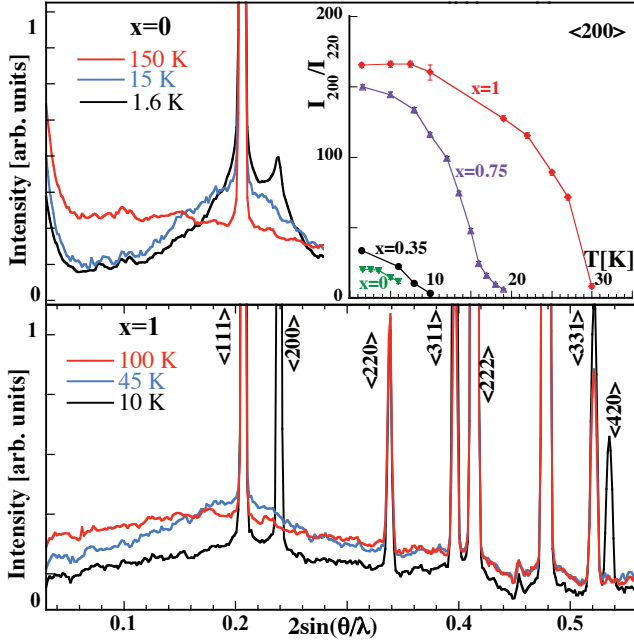


FIG. 1: (Color online) DMC patterns of $x=0$ and $x=1$ samples at selected temperatures. Reasonable statistics on diffuse scattering has been obtained by measuring for about 10 h at one temperature. Inset: Temperature dependence of intensity of the $\langle 200 \rangle$ magnetic reflection normalized to the nuclear $\langle 220 \rangle$ intensity.

for four compositions have been collected in the temperature range 1.5 K - 150 K on the DMC instrument at SINQ with a neutron wavelength $\lambda=2.4526 \text{ \AA}$. Broad bumps resembling a liquid-like structure factor due to short-range magnetic order start to develop near 100 K; they narrow and shift to higher $\sin\theta/\lambda$ with cooling (Fig. 1). Ap-

TABLE I: The Néel temperature, T_N , and the 1.6 K ordered magnetic moment, M , determined from the DMC patterns.

x	T_N [K]	M [μ_B]
1.0	29	3.53(3)
0.75	16.5	2.59(3)
0.35	9	1.31(4)
0.0	5	0.25(7)

proaching T_N the diffuse scattering localizes near the $\langle 111 \rangle$ and $\langle 200 \rangle$ positions. Below T_N the liquid-like features remain but gradually loose spectral weight as the magnetic Bragg peaks due to long-range order develop. The amount of maximal diffuse scattering is continuously increasing from Co_3O_4 to CoAl_2O_4 (Fig. 2). We can quantify it by an area of Lorentzian fitted to the first diffuse bump. As shown in the inset of Fig. 2 this area is largest roughly at $T/T_N \approx 1$ for all compositions, but for $x=0$ and $x=0.35$ diffuse scattering develops far above and remains significantly below this value yielding extended temperature interval of the spin-liquid phase. For $x=1$ the T/T_N interval revealing diffuse scattering is narrower resembling the regime of critical scattering observed in frustrated systems near phase transitions.

Regarding the long-range order, all samples show magnetic Bragg peaks at low temperatures. The ordering temperature T_N and the static ordered magnetic moment decrease from Co_3O_4 to CoAl_2O_4 (see Table I and inset of Fig. 1). It should be noted that the $x=0$ diffraction pattern does not correspond to a conventional long-range ordered state: diffuse scattering clearly dominates and the $\langle 200 \rangle$ peak is so broad and weak that the ordered moment cannot be determined with high accuracy. Nevertheless, the magnetic Bragg pattern is the same for all compositions and it is consistent with the collinear two-sublattice model proposed by Roth⁸.

To model the observed magnetic diffuse scattering we used the quasistatic approximation¹⁶, which assumes that all observed diffuse scattering can be attributed to static correlations. This approach is justified as the bandwidth of magnetic excitations is below 6 meV^{7,17} and all scattering with energies below 14.7 meV is summed in our diffraction experiment. We performed a Monte-Carlo search for the ground state of a cluster of 1047 atoms. The energy of the classical Heisenberg Hamiltonian for spins \mathbf{S} interacting with first- and second-neighbour antiferromagnetic couplings $J_1, J_2 > 0$

$$H = J_1 \sum_{\langle ij \rangle} \mathbf{S}_i \cdot \mathbf{S}_j + J_2 \sum_{\langle\langle ij \rangle\rangle} \mathbf{S}_i \cdot \mathbf{S}_j \quad (1)$$

was minimized. The moments were kept equal and constant in magnitude; their direction was changed at random, one at the time, and to obtain the ground state only energy-decreasing moves were accepted. The stopping criterion for the Monte-Carlo was that the last 1000 accepted configurations had an energy spread less than $10^{-6} J_1$. Runs have been repeated for the whole range

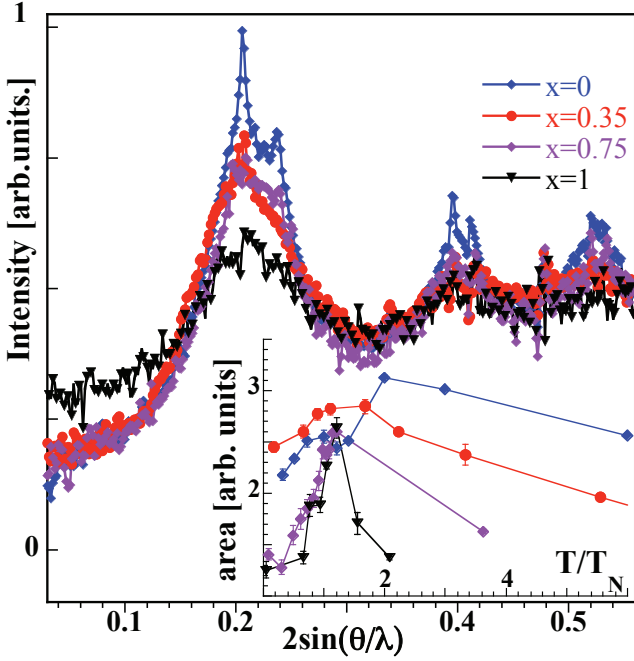


FIG. 2: (Color online) Maximal diffuse magnetic scattering in the differential T-150 K neutron powder patterns. The T-value is equal to 6, 15, 19, 45 K for the compositions $x=0, 0.35, 0.75$ and 1, respectively. Inset: Evolution of diffuse scattering quantified as an area of Lorentzian fitted to the first bump.

$0 \leq J_2/J_1 \leq 1$. We calculated the static spin-pair correlation functions and diffraction patterns for the Monte-Carlo ground state (MCGS) and the reference AFM clusters for each J_2/J_1 . The correlation function is given by

$$CF(d) = \frac{2}{3} \sum_{ij} \mathbf{S}_i \cdot \mathbf{S}_j \delta(|r_i - r_j| - d) \quad (2)$$

where d is the distance between spins at positions r_i and r_j . We found that for the range $0 < J_2/J_1 < 1/8$ the collinear AFM is the ground state, in agreement with Ref. 3. However, the MCGS lies within at most $10^{-6} J_1$ from it (Fig. 3 inset). Analytical calculations confirm these results¹⁸. Interestingly the energy minimum corresponding to the ground state is very flat, as a lot of configurations have very close energies. This is expected for a strongly frustrated system.

The MCGS is closely related to the collinear AFM state, but progressively departs from it with increasing J_2/J_1 . This is clearly seen in the decay of spin correlations, which can be quantified by the ratio CF_{MCGS}/CF_{AFM} . In Fig. 3 we plot $\log|CF_{MCGS}/CF_{AFM}|$ versus squared distance d^2 between spins. Near $J_2/J_1=1/8$ the decay changes from predominantly Gaussian $e^{-1/2 \cdot (d/w)^2}$ (a straight line in this choice of axes) to a mixed Gaussian-exponential form $e^{-d/L} \cdot e^{-1/2 \cdot (d/w)^2}$ (a curve bending downwards for $200 < d^2 < 400 \text{ \AA}^2$). This behaviour can be attributed to the incipient spiral surface. In the calculated diffraction patterns (Fig. 4, top) these changes

are evidenced as progressive broadening and distortion of Bragg peaks. For $J_2/J_1 > 0.5$ the correlations are completely changed and features of the collinear AFM state fade out.

To evaluate J_2/J_1 for the $\text{Co}(\text{Al}_{1-x}\text{Co}_x)_2\text{O}_4$ system we

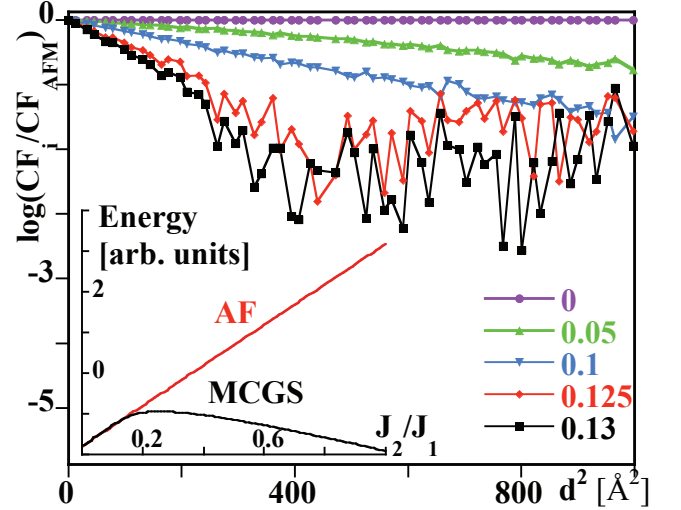


FIG. 3: (Color online) Log of ratio of spin-pair correlation functions $|CF_i/CF_{AFM}|$ versus d^2 for selected J_2/J_1 ratios. Inset: The minimal energy curve for the collinear antiferromagnet (red) and for the best Monte-Carlo ground state (black).

compared the experimental and calculated diffuse scattering. The patterns shown in Fig. 2 were obtained as differences between data measured at $T=6, 15, 19$ and 45 K (for $x=0, 0.35, 0.75$ and 1 , respectively) and 150 K . In the calculated patterns we had to include a finite J_3 to overcome the additional frustration arising from thermally occupied excited states to obtain the ordered AFM state at $T < T_N$. The MC procedure was now changed, allowing for system equilibrations at different temperatures. All moves that would decrease the energy or that would increase it with probability $\propto e^{-\Delta E/T}$ were accepted¹⁹. When the average and fluctuations of the energy of a large number of the last accepted states were sufficiently stable the temperature was changed. Fixing $J_1=1$ as a convenient energy scale, J_2, J_3 or T were varied, each in several steps.

Very good fits have been obtained for all samples studied when comparing with the MC results for $J_2/J_1 \approx 0.12$ at $T \approx 0.7J_1$ ²¹. As examples we present the results for CoAl_2O_4 and Co_3O_4 in Fig. 4 (bottom). As for this ratio the ground state is the collinear AFM and not the degenerate spiral ground state, the general term 'spin-liquid' and not 'chiral spin-liquid' is appropriate for the high-temperature regime above T_N in the title system.' A constant ratio J_2/J_1 for all compositions disagrees with the previous findings¹⁴ that CoAl_2O_4 and Co_3O_4 are significantly different due to change in J_2/J_1 . Our results suggest that it is the overall energy scale, J_1 (and with it J_2), which changes as a function of x . We find ad-

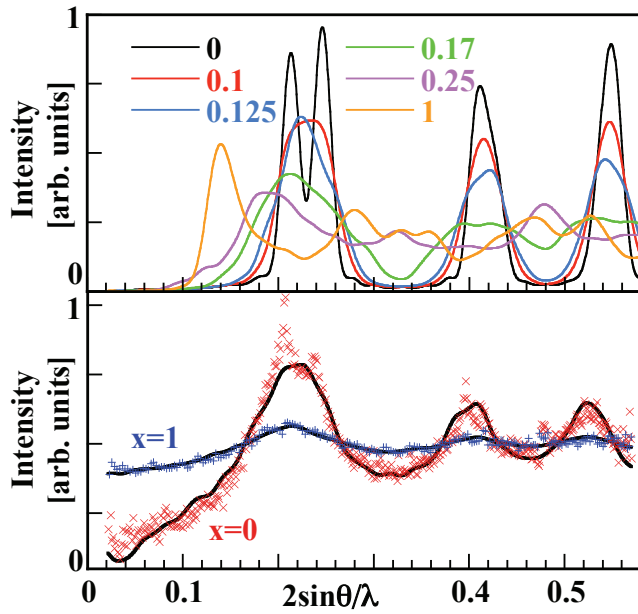


FIG. 4: (Color online) Top: Calculated powder diffraction patterns for several selected J_2/J_1 ratios at $T = 0$ K. Bottom: Observed (symbols) and calculated (line) powder diffraction patterns for $x=0$ and $x=1$ corresponding to the best model parameters $J_2/J_1=0.12$, $J_3/J_1=0.01$, $T/J_1=0.7$. The calculated patterns are corrected for the magnetic form factor of Co^{3+} and polynomial background.

ditional confirmation in the temperature dependence of the diffuse scattering. The scattering for $x=1$ at $T=32$ K is identical to that of $x=0$ in the 1.6 K- 5 K range. Thus the magnetic configurations - or at least their pair correlations - are identical for the two compositions at two different temperatures. The change of the overall energy with substitution apparently originates from the peculiarities of the electronic structure. Band structure analysis²⁰ shows that near the Fermi level in Co_3O_4 there

are Co^{3+} d and oxygen p states, while in CoAl_2O_4 the Al p states are absent near the Fermi level and the weight of O p is diminished. This implies that the interaction path $\text{O}-\text{Co}^{3+}-\text{O}$ is more effective and the corresponding exchange integrals are larger in Co_3O_4 .

Our findings imply that the μSR results⁹ on Co_3O_4 should be explained rather by short-range correlations than by incommensurate magnetic order. Also, based on the position of CoAl_2O_4 in the J_2/J_1 phase diagram, we suggest that even in an ideal sample, with no inversion or other perturbation, the ground state would be collinear, though one might need very low temperatures to reach it²². We remark that the elaborated approach to fit measured diffuse magnetic neutron scattering to Monte-Carlo simulations can be easily adapted to other frustrated systems and would be useful in justification of an anticipated Hamiltonian.

In summary we studied the evolution of magnetic states in $\text{Co}(\text{Al}_{1-x}\text{Co}_x)_2\text{O}_4$ polycrystalline samples with temperature and substitution in the B-site. We observed short-range and long-range order for all compositions. Employing Monte-Carlo simulations we found that the system is in the vicinity of the critical point $J_2/J_1=1/8$, where the spiral spin-liquid develops³, but stays in the weakly frustrated limit. We also found that replacement in the nonmagnetic B-site changes the strength of exchange interactions which in turn leads to significant differences in the ordering temperatures and in the extent of the spin-liquid regime.

We thank the expert experimental assistance of L. Keller and D. Sheptyakov. The work was performed at SINQ and SLS, Paul Scherrer Institute, Villigen, Switzerland. The support of PSI via the collaborative grant MOP1-33010-CH-08 of the GAP of the US CRDF is gratefully acknowledged. NBC acknowledges the support by the Danish Natural Science Research Council under DAN-SCATT.

* e-mail: Oksana.Zaharko@psi.ch

- ¹⁵ Spin-liquid is characterized by rapid (at least exponential) decay of spin-spin correlations and the correlation length does not exceed the interatomic distance², which result in a spin liquid-like structure factor.
- ² B. Canals, C. Lacroix PRL **80**, 2933(1998).
- ³ D. Bergman, J. Alicea, E. Gull, S. Trebst, L. Balents, Nature Physics **3**, 487(2007).
- ⁴ J.-S. Bernier, M. J. Lawler, Y. B. Kim, Phys. Rev. Lett. **101**, 047201 (2008).
- ⁵ V. Fritsch, J. Hemberger, N. Büttgen, E.-W. Scheidt, H.-A. Krug von Nidda, A. Loidl, V. Tsurkan, Phys. Rev. Lett. **92**, 116401 (2004).
- ⁶ A. Krimmel, M. Mücksch, V. Tsurkan, M. M. Koza, H. Mutka, C. Ritter, D. V. Sheptyakov, S. Horn, A. Loidl, Phys. Rev. B **73**, 014413 (2006).
- ⁷ A. Krimmel, H. Mutka, M. M. Koza, V. Tsurkan, A. Loidl,

- Phys. Rev. B **79**, 134406 (2009).
- ⁸ W. L. Roth, J. Phys. Chem. Solids **25**, 1(1964).
- ⁹ Y. Ikeda, J. Sugiyama, H. Nozaki, H. Itahara, J. H. Brewer, E. J. Ansaldo, G. D. Morris, D. Andreica, A. Amato, Phys. Rev. B **75**, 054424 (2007).
- ¹⁰ W. L. Roth, Le Journal de Physique **25**, 507(1964).
- ¹¹ A. Krimmel, V. Tsurkan, D. Sheptyakov, A. Loidl, Physica B **378-380**, 583 (2006).
- ¹² N. Tristan, J. Hemberger, A. Krimmel, H. A. Krug von Nidda, V. Tsurkan, A. Loidl, Phys. Rev. B **72**, 174404 (2005).
- ¹³ T. Suzuki, N. Nagai, M. Nohara, H. Takagi, J. Phys.: Condens. Matter **19**, 145265 (2007).
- ¹⁴ N. Tristan, V. Zestrea, G. Behr, R. Klingeler, B. Büchner, H. A. Krug von Nidda, A. Loidl, V. Tsurkan, Phys. Rev. B **72**, 094412 (2008).
- ¹⁵ Vegard's law is an approximate empirical rule defining a

linear relation between the lattice constant and the concentrations of the constituent elements at constant temperature.

¹⁶ van Hove Phys. Rev. **95**, 1374 (1954).

¹⁷ Results of recent inelastic neutron scattering (INS) experiments, to be published.

¹⁸ A. Cervellino to be published.

¹⁹ $\Delta E = E_{last\ trail} - E_{last\ accepted}$

²⁰ A. Walsh, S.-H. Wei, Y. Yan, M. M. Al-Jassim, J. A.

Turner, M. Woodhouse, B. A. Parkinson, Phys. Rev. B **76**, 165119 (2007).

²¹ The difference between the calculated powder diffraction patterns for $J_2/J_1=0.12$ and 0.125 is minor. We reinforce our powder results by INS experiment¹⁷.

²² Analysis of the INS data to extract the absolute values of J_1, J_2 and to validate our conclusions is in progress.